Sixth International Symposium on Turbulence and Shear Flow Phenomena
Seoul, Korea, 22-24 June 2009

LARGE-SCALE COHERENT STRUCTURES IN ROUGH-BED TURBULENT OPEN-CHANNEL FLOW

Jianmin Ma
Department of Engineering
Queen Mary, University of London
Mile End Road, London E1 4NS, UK
j.m.ma@qmul.ac.uk

J.J.R.Williams
Department of Engineering
Queen Mary, University of London
Mile End Road, London E1 4NS, UK
j.j.r.williams@qmul.ac.uk

ABSTRACT

This paper reports the results obtained from a Direct Numerical Simulation (DNS) regarding the large-scale coherent structures in turbulent open-channel flow with a rough bed. The gravel bed is represented by a hexagonal arrangement of spheres with a diameter of a quarter of flow depth. The length of the structures are shown to be longer than the computational box, roughly 10 times the effective flow depth, and the width tends to be one order of magnitude smaller than the length. The parallel meandering structures mainly locate in the inter-mediate region of the channel and are composed of a group of quasi-streamwise vortices and asymmetric hairpin vortices, with signatures of elongated local maximum of streamwise velocity in the middle. It is also found that these structures contribute substantially to both of the Reynolds Stress (RS) and Turbulent Kinetic Energy (TKE).

INTRODUCTION

The dynamics of coherent structures in turbulent flows have been studied extensively over the past few decades. More recently, the nature of large-scale coherent structures was explored by different groups. The structures are mostly observed to be composed of hairpin vortex packets (Tomkins et al. 2003, Ganapathisubramani et al. 2003) and identified according to their velocities, length and time scales as younger packets, older packets and even older packets from upstream (Adrian et al. 2000) or primary, secondary, tertiary and downstream hairpin vortices (Zhou et al. 1999). The small vortices increase and connect with each other along the distance away from the wall and develop into much larger structures (Zhou et al. 1999).

The length of the large structures is shown to be approximately two to three times flow depth and width to be one-order magnitude smaller in turbulent boundary layer (Ganapathisubramani et al., 2003; Adrian et al., 2000) and channel flow (DEL Alamo et al. 2006, Hurther et al. 2007). In pipe flow, the wavelength of very large scale motion, aligned by large scale packets, can be more than 8~16 pipe radii (Kim and Adrian, 1999; Guala et al., 2006). Moreover, these large coherent structures are demonstrated to contribute substantially to Reynolds stress (Ganapathisubramani et al., 2003; Guala et al. 2006), mean shear and turbulent kinetic energy (Hurther et al. 2007) and showed Reynolds number similarity (Guala et al. 2006).

In the structure model proposed by Adrian et al. (2000), the hairpin packets originate from the wall due to some kind of disturbance, then intensified to be an omega-shape structure, and may also induce a secondary hairpin if the primary structure is strong enough. The hairpin vortex is basically asymmetric and also associated with the bulges in the outer space. The angle of the vortex head ranges from 15^0 to 75^0, as a function of the distance from the wall. One important feature is that the structures can break down and reconnect as indicated from their simulation data.

Tomkins and Adrian (2003) revealed the spanwise growth mechanism of the hairpin structures. In their model the spanwise structure grows self-similarly in a general sense, though not strictly, from the evidence of linear increase of the spanwise length away from the wall. This concept does help to explain the merging of the streaks although it does not support the growth of long low-speed region. The hairpin packets are organized along the streamwise direction in the logarithmic region, characterised by the large-scale momentum deficit. The packet merging evidence is the stagnation point together with the spanwise distribution of two low momentum regions with a high momentum region in the middle.

In the experimental study of Liu et al. (2001), the large-scale motion with length scale larger than 3.2h contains half of the turbulent kinetic energy and also more than two thirds of the Reynolds Stress. They suggest the streamwise length scale in channel flow could be as long as the pipe flows. Zhou et al. (1999) investigated the evolution of a single hairpin in the channel flow by DNS. The initial structure obtained from a linear stochastic estimation procedure develops into a hairpin structure first, which is shown to be independent of the initial

strength and initial location of the event vector. Then, the hairpin vortex evolves into an omega shaped vortex and produces secondary, tertiary and downstream vortices. Quasi-streamwise vortices on the sides of the vortex structure are observed. This autogeneration mechanism reasonably explains the formation of the hairpin packets and should be applied to channel flow with different bed roughness and Reynolds number.

In the numerical study of DEL Alemo et.al (2006), two kinds of clusters are observed: one is small vortex packets detached from the wall; the other is tall clusters attached to the wall. The low streamwise velocity motion is considered to be the wakes of the clusters and the clusters on the other hand, are produced by the wakes. This dynamic process offers another model for the structure organization in the turbulent flow.

Despite great process achieved regarding the characteristic of large-scale motions in turbulent flow, the merging of long streaks, usually appear as elongated and meandering features, is still not clear. The objective of this paper is to get a better understanding of the large scale coherent structures in turbulent open-channel flow with a rough bed by DNS. The paper is organized as follows. The numerical technique is described in the following section. Then, the results, including the features of the coherent structures, variation of Reynolds Stress and Turbulent Kinetic Energy, are addressed and compared with previous works. A brief conclusion is presented in the final section.

METHODOLOGY

We carried out a direct numerical simulation of the turbulent open-channel flow over a rough-bed. The gravel bed is represented by a hexagonal arrangement of fixed spheres with the diameter of a quarter of flow depth, d. The length scale of the numerical box is $4\sqrt{3}d$ in the streamwise direction and $4d$ in the spanwise direction. We employed no-slip and no penetration conditions on sphere surface and stress-free hard lid for channel top surface. A parallel complex-geometry code was performed in this simulation. Periodic boundary conditions are used in both horizontal directions. The flow Reynolds number $Re^+(Re^+=u_\tau d/\nu)$ is 533 and the roughness Reynolds number $k_s^+(k_s^+= k_s u_\tau/\nu)$ is 100 so that the bed is fully rough.

The incompressible turbulent flow is governed by the Navier-Stokes equations and the continuity equation

$$\frac{\partial u_i}{\partial t}+\frac{\partial (u_i u_j)}{\partial x_j}=-\frac{1}{\rho}\frac{\partial p}{\partial x_i}+\nu\frac{\partial^2 u_i}{\partial x_j x_j}+b_i \qquad (1)$$

$$\frac{\partial u_i}{\partial x_i}=0 \qquad (2)$$

In the above equations, u_i are the velocity components, t is time, ρ is the fluid density, p is the pressure, ν is the kinematic viscosity, b_i are the body force components. Axes x, y, z represent streamwise, vertical and spanwise directions respectively and, the center of reference frame is located at the bottom of channel.

In the simulation, staggered grid with a second order finite difference method is used for spatial discretization and a second order Adams-Bashforth method for time integration. A ficitus domain multigrid preconditioner with a conjugate gradient method is used for Poisson pressure equation. The simulation was performed as LES for about 30 letot (large eddy turnover time) first to establish a fully developed turbulent flow field. Then, simulation was continued using DNS grid until statistically steady, by checking the total shear stress profile. We employ a Cartesian grid of resolution of $1024\times512\times128$ for $4\sqrt{3}d\times4d\times d$, with grid sizes of 3.6 wall units, 4.2 wall units and 4.2 wall units in x, y, z directions respectively. The kolmogorov length scale is approximately 3.0 wall units. More details regarding the simulation can be found in Singh, Sandham and Williams (2007).

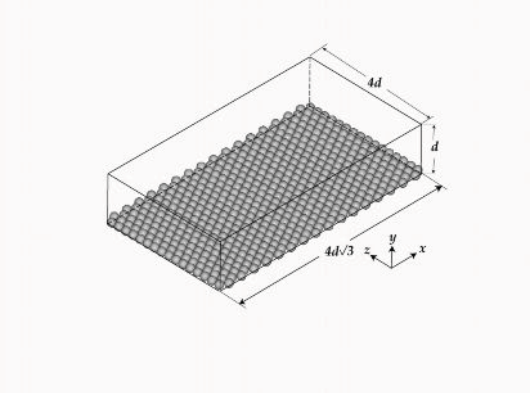

Figure 1: Geometry of DNS

RESULTS AND DISCUSSIONS

We use Q-approach (Hunt et al., 1988) to visualize the coherent structures obtained in DNS. As shown in Fig.2 and Fig.3, both of the instantaneous data contain three parallel large-scale structures. The experimental work of Roy et al. (2004) states that the length of the large motions is 3 to 5 times flow depth and the width is 0.5 to 1 times flow depth in a gravel-bed river. The length of the structure is hard to estimate from the data here as the computational box is not big enough to tell how long exactly the structures are. But it is simply larger than about 10 times the effective flow depth. The width is roughly the same as their experimental result. The structures are meandering and adjacent, which makes the identification of the structures from each other difficult. As observed by many other researchers (Robinson, 1991; Zhou et al, 1999), the asymmetric hairpin vortices with one leg are more frequently generated than the symmetric hairpin vortices. As a consequence, the long structures are mainly composed of quasi-streamwise vortices and asymmetric hairpin vortices with single leg.

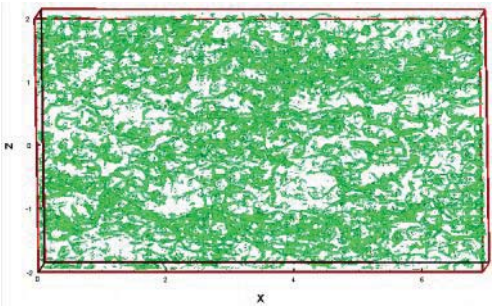

Figure 2: Instantaneous large-scale coherent structures: Q = 0.0098$Q_{max.}$

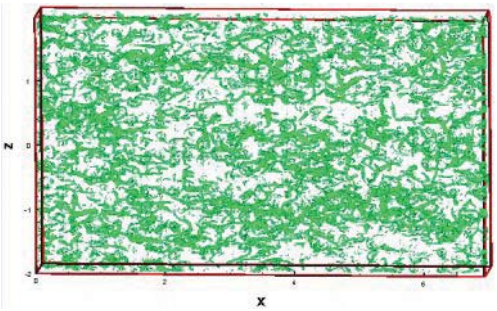

Figure 3: Instantaneous large-scale coherent structures: Q = 0.0149$Q_{max.}$

Fig.4 and Fig.5 indicate the growth of the structures along the depth of flow. The signature of the structure is the local maximum of streamwise velocity. This implies that the organization of the coherent structures is different from the hairpin vortex model proposed by Tomkins and Adrian (2003) with low momentum region in the center. Fig.6 shows that the high velocity region originates from the counter-rotating vortex pairs. The dashed lines indicate the high velocity region corresponding to the streamwise velocity contour in Fig.5, with vortex pairs on both sides of the region. The rotating direction of the vortices is different with the hairpin packets model. As shown in Fig.7, the left counter-rotating vortex pairs, which can increase the local streamwise velocities, tend to aggregate together to form the large-scale coherent structures as observed here; whilst the right vortex pairs, which decreases the local streamwise velocities, are easily separate by the main stream, unless they are strong enough to suffer the shear stress.

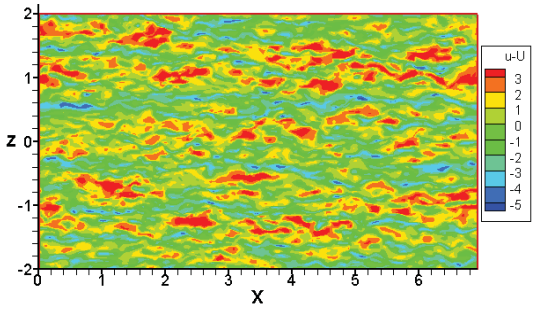

Figure 4: Fluctuating streamwise velocity contour at y = 0.28d.

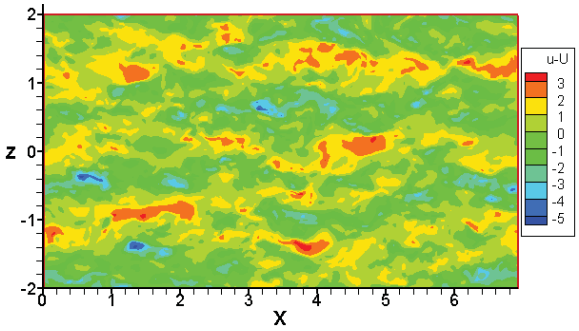

Figure 5: Fluctuating streamwise velocity contour at y = 0.56d.

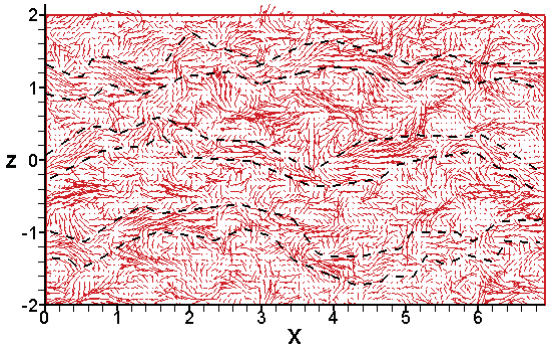

Figure 6: Horizontal velocity vector plot at y = 0.56d.

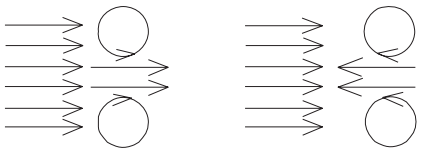

Figure 7: Different patterns of counter-rotating vortex pairs of large coherent structures.

Fig.8 shows the organization of the structures: small and short quasi-streamwise vortices at the bottom whilst larger and longer quasi-streamwise vortices or asymmetric hairpin vortices far away from the wall. This is consistent with the observation of Tomkins (2003) as the vortex core increases away from the wall. Consequently, the wider region between the vortices and also between the structures explains the growth of the high-speed and low-speed streaks perfectly.

Fig.9 depicts the uniform streamwise momentum region retarded by the large structures, as observed by Adrian et al. (2000) and Hurther et al. (2007). The circles in the figure denote the head of the hairpin vortices, with tilt angles range from 10^0 to 60^0 approximately, in agreement with the results of Adrian et al. (2000).

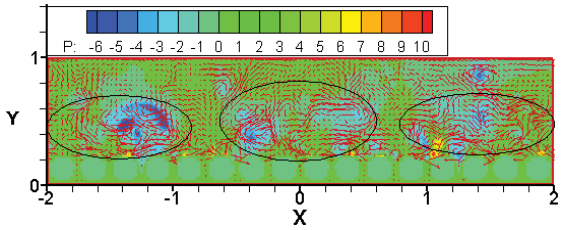

Figure 8: Spanwise velocity vector and pressure plot.

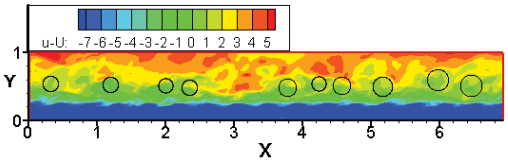

Figure 9: Uniform streamwise momentum.

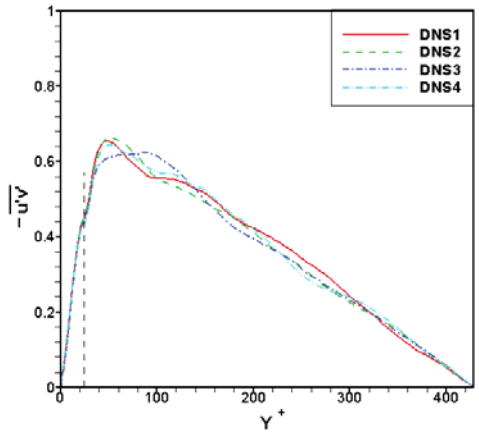

Figure 10: Instantaneous Reynolds Stress, normalized by bed shear velocity (dashed line denotes top of spheres).

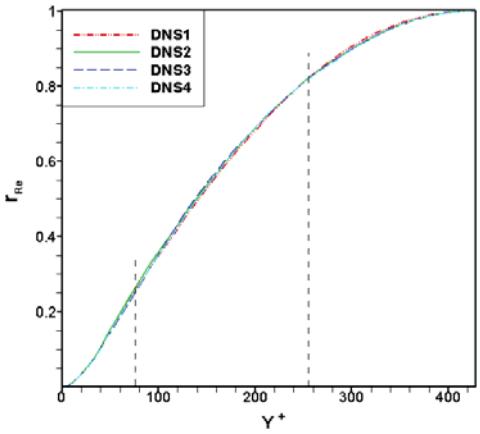

Figure 11: Instantaneous cumulative Reynolds Stress (dashed lines denote three sub-regions of the channel) .

We divide the channel into three sub-regions as Nezu (1993): wall region [y/h < (0.15~0.2)], intermediate region [(0.15~0.2) ≤ y/ h ≤ 0.6], and free-surface region (0.6< y/h ≤ 1.0). The wall region corresponds to the "Inner layer" of boundary layer flow whilst the intermediate and free-surface regions are outer layer. We take the flow depth as the effective flow depth, which originates from the effective bed level.

Fig.10 shows the variation of the Reynolds Stress along the flow depth. As argued by Hutchins et al. (2007), the local instantaneous Reynolds Stress can be activated by the superstructures. The fluctuations of Reynolds Stress beneath the structures are clearly observed. But the cumulative Reynolds Stress keeps constant in Fig.11. This implies the large structures actually not only influence the Reynolds Stress beneath them, also above them. In consequence, the ratio of contributions from different regions to the total remains the same.

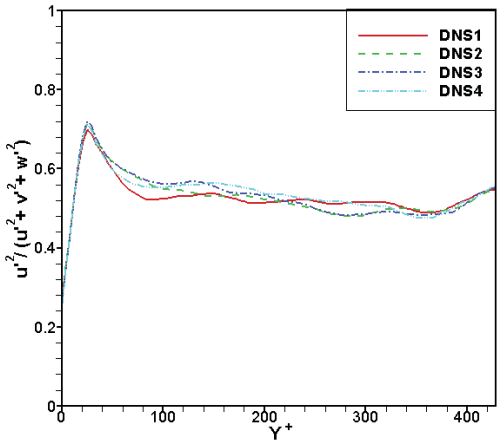

Figure 12: Contributions of *u'* to total TKE.

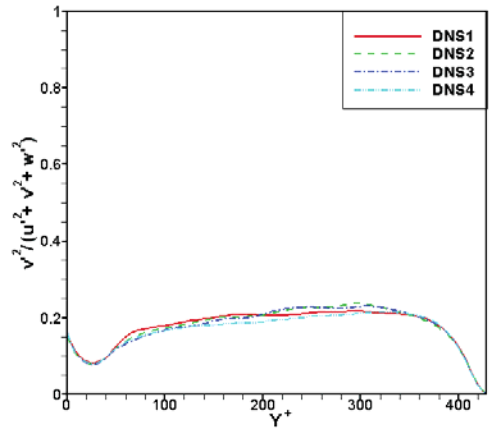

Figure 13: Contributions of *v'* to total TKE.

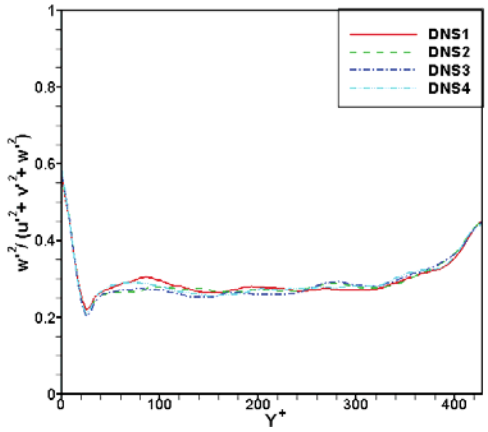

Figure 14: Contributions of *w'* to total TKE.

Fig.12~14 indicate the variation of the contributions of fluctuating velocity components to the total Turbulent Kinetic Energy along with flow depth. More than 50% of the energy comes from *u'*, whilst about 30% from *w'*. The *u'* contribution decreases from the top of spheres, all the way through the intermediate region, finally increases in the surface region. This corresponds with the uniform streamwise momentum retarded by the structures in Fig.9. The *v'* contribution increases gradually from the wall region until the free surface, where the large structures disappear. This implies the large structures can activate the vertical fluctuating velocities, which can be understood from the large area of high-speed upwash and downwash fluid between the vortex pairs in Fig.8. The *w'* contribution remains stable in the intermediate region and increase sharply near the top of channel. This is presumably due to the deactivation of the large structures.

CONCLUSIONS

We carry out a DNS of turbulent open-channel flow with a rough bed concerning the characteristics of the large-scale coherent structures. Our model explains the merging of the streaks from near-wall region to the outer region as observed by many other studies, which cannot be explained by the hairpin packets mechanism or wake model. The majority of the structure locates in the intermediate region of the channel whilst the head of the hairpin vortices can reach the free-surface region and the small quasi-streamwise vortices grow from the wall region. The length of the meandering structures can be larger than the length of the computational domain, and the width is between ½ to 1 effective flow depth. The structures are composed of small quasi-streamwise vortices at the bottom, larger quasi-streamwise vortices and asymmetric hairpin vortices above. The signature of the structures is the high streamwise velocity region created by the counter-rotating vortex pairs. The elongated high speed and low speed regions can explain the growth of the streaks along with the flow depth perfectly. The influence of the structures on Reynolds Stress and Turbulent Kinetic Energy can be observed over the entire channel. Future work includes studies of the development of the large-scale structures and the exact length scale in the streamwise direction.

ACKNOWLEDGEMENTS

This work is supported by UK Turbulence Consortium for the computing support. The authors also wish to thank the reviewers for their suggestions.

REFERENCES

Adrian, R. J., Meinhart, C. D. and Tomkins, C. D. (2000). "Vortex organization in the outer region of the turbulent boundary layer." *J. Fluid Mech.,* 422, 1-54.

Del Alamo, J. C., Jimenez, J., Zandonade, P. and Moser, R. D. (2006). "Self-similar vortex clusters in the turbulent logarithmic region." *J. Fluid. Mech.*, 561, 329-358.

Ganapathisubramani,B.,Hutchins,N.,Hambleton, W. T., Longmire, E. K. and Marusic, I. (2005). "Investigation of large-scale coherence in a turbulent boundary layer using two-point correlations." *J. Fluid. Mech.,* 524, 57-80.

Guala, M. G., Hommema, S. E. and Adrian, R. J. (2006). "Large-scale and very-large-scale motions in turbulent pipe flow." *J. Fluid. Mech.,* 554, 521-542.

Hunt, J. C. R., Wary, A. A. & Moin, P. (1988). "Eddies, stream, and convergence zones in turbulent flows." *Center for turbulence Research Report CTR*-S88, p.193.

Hurther, D., Lemmin, U. and Terray, E.A. (2007). "Turbulent transport in the outer region of rough-wall open-channel flows: the contribution of large coherent shear stress structures (LC3S)." *J. Fluid. Mech.,* 574, 465-493.

Jimenez, J., Del Alamo, J. C. and Flores, O. (2004). "The large-scale dynamics of near-wall turbulence." *J. Fluid. Mech.,* 505, 179-199.

Kim, K. C. and Adrian R. J. (1999). "Very large-scale motion in the outer layer." *Phys. Fluids*, 11, 417-422.

Liu, Z., Adrian, R. J. and Hanratty, T. J. (2001). "Large-scale modes of turbulent channel flow: transport and structure." *J. Fluid. Mech.,* 448, 53-80.

Nezu, I. and Nakagawa, H. (1993). "*Turbulence in Open-Channel Flows*." Balkema, Rotterdam.

Robinson, S. K. (1991). "Coherent motions in the turbulent boundary layer." *Annu. Rev. Fluid. Mech.*, 23, 601-639.

Roy, A. G., Buffin-Belanger, T., Lamarre, H. and Kirkbride, A. D. (2004). "Size, shape and dynamics of large-scale turbulent flow structures in a gravel-bed river." *J. Fluid. Mech.,* 500, 1-27.

Singh, K. M., Sandham, N. D. and Williams, J. J. R. (2007). "Numerical simulation of flow over a rough bed." *J. Hydr. Engrg.,* 133(4), 386-398.

Tomkins, C. D. and Adrian R. J. (2003). "Spanwise structure and scale growth in turbulent boundary layers." *J. Fluid. Mech.,* 490, 37-74.

Zhou, J., Adrian, R. J., Balachandar, S. and Kendall, T. M. (1999). "Mechanisms for generating coherent packets of hairpin vortices in channel flow." *J. Fluid. Mech.,* 387, 353-396.